

Product Datasheet

ABCA1 Antibody - BSA Free NB400-105

Unit Size: 0.1 ml

Store at 4C short term. Aliquot and store at -20C long term. Avoid freeze-thaw cycles.

www.novusbio.com



technical@novusbio.com

Reviews: 7 Publications: 398

Protocols, Publications, Related Products, Reviews, Research Tools and Images at:
www.novusbio.com/NB400-105

Updated 12/20/2023 v.20.1

**Earn rewards for product
reviews and publications.**

Submit a publication at www.novusbio.com/publications

Submit a review at www.novusbio.com/reviews/destination/NB400-105



NB400-105

ABCA1 Antibody - BSA Free

Product Information	
Unit Size	0.1 ml
Concentration	1 mg/ml
Storage	Store at 4C short term. Aliquot and store at -20C long term. Avoid freeze-thaw cycles.
Clonality	Polyclonal
Preservative	0.02% Sodium Azide
Isotype	IgG
Purity	Immunogen affinity purified
Buffer	PBS
Target Molecular Weight	220 kDa
Product Description	
Host	Rabbit
Gene ID	19
Gene Symbol	ABCA1
Species	Human, Mouse, Rat, Porcine, Canine, Chicken, Chinese Hamster, Equine, Hamster, Mustelid, Primate, Rabbit
Reactivity Notes	Canine reactivity reported in scientific literature (PMID: 24612239). Rabbit reactivity reported in scientific literature (PMID: 26444796). Chinese Hamster reactivity reported in scientific literature (PMID: 27902765). Primate reactivity reported in scientific literature (PMID: 25440061). Equine reactivity reported in scientific literature (PMID: 26711702).
Immunogen	Partial peptide sequence (within residues 1100-1300) of human ABCA1 Antibody [UniProt# O95477]. Actual immunogen sequence is proprietary information.
Product Application Details	
Applications	Western Blot, Simple Western, Chromatin Immunoprecipitation, ELISA, Flow Cytometry, Gel Super Shift Assays, Immunoblotting, Immunocytochemistry/Immunofluorescence, Immunohistochemistry, Immunohistochemistry-Frozen, Immunohistochemistry-Paraffin, Immunoprecipitation, Block/Neutralize, Chromatin Immunoprecipitation (ChIP), Dual RNAscope ISH-IHC, Gel Supershift Assay, Knockdown Validated, Knockout Validated, PCR
Recommended Dilutions	Western Blot 1:500, Simple Western 1:50, Chromatin Immunoprecipitation reported in scientific literature (PMID 19515742), Flow Cytometry 1:400. Use reported in scientific literature (PMID 21501868), ELISA reported in scientific literature (PMID 18541924), Immunohistochemistry 1:200, Immunocytochemistry/ Immunofluorescence 1:100. Use reported in scientific literature (PMID 21501868), Immunoprecipitation 1:10-1:500. Use reported in scientific literature (PMID 21846716; 21106520), Immunohistochemistry-Paraffin 1:200, Immunohistochemistry-Frozen, Immunoblotting reported in scientific literature (PMID 27599291), Gel Super Shift Assays reported in scientific literature (PMID 15684432), Gel Supershift Assay, Chromatin Immunoprecipitation (ChIP), Knockout Validated reported in scientific literature (PMID 32273567), Knockdown Validated reported in scientific literature (PMID 31666189), Block/Neutralize reported in scientific literature (PMID 30821416), PCR reported in scientific literature (PMID 27406916), Dual RNAscope ISH-IHC

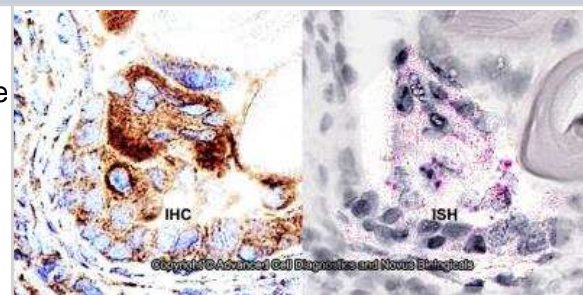


Application Notes

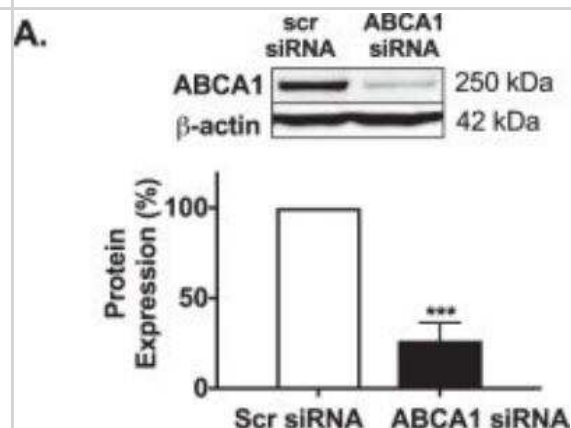
Western Blot band representing ABCA1 is observed at approx. 220 kDa. Additional non-specific bands are seen at lower molecular weights, but do not interfere with the ABCA1 signal. In Simple Western only 10-15 uL of the recommended dilution is used per data point. Separated by Charge.

Images

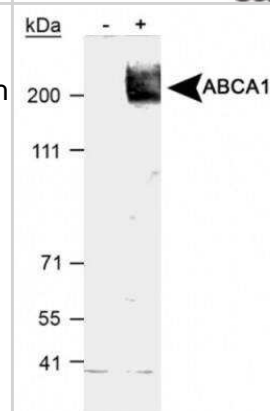
Formalin-fixed paraffin-embedded tissue sections of human prostate cancer were probed for ABCA1 mRNA (ACD RNAScope Probe, catalog # 432291; Fast Red chromogen, ACD catalog # 322360). Adjacent tissue section was processed for immunohistochemistry using rabbit polyclonal (Novus Biologicals catalog # NB400-105) at 1.5ug/mL with overnight incubation at 4 degrees Celsius followed by incubation with anti-rabbit IgG VisUCyte HRP Polymer Antibody (Catalog # VC003) and DAB chromogen (yellow-brown). Tissue was counterstained with hematoxylin (blue). Specific staining was localized to glandular cells.



HSKMCs were transfected with scrambled siRNA (scr siRNA) or ABCA1 siRNA. The cells were lysed and ABCA1 (A) protein levels were quantified by immunoblotting. Image collected and cropped by CiteAb from the following publication (<https://www.nature.com/articles/s41598-018-38014-3>) licensed under under a CC-BY license.



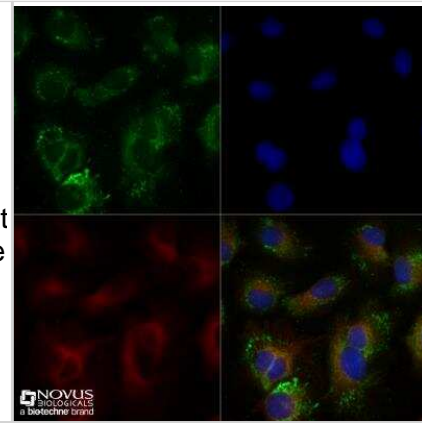
Analysis of ABCA1 in total cell lysates of RAW264.9 cells treated with vehicle (-) or 9-cisretinoic acid and 22Rhydroxycholesterol (+). Samples used for this testing were 40 ug of total cell post-nuclear lysate from each group.



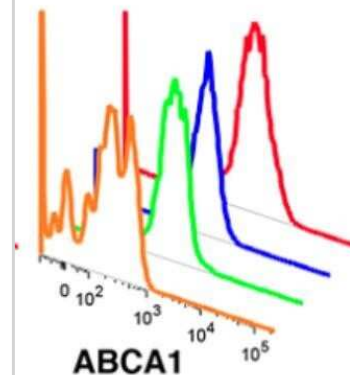
HepG2 cells were grown to 60% confluency, serum starved for 24 hours, and then treated with 1uM TO9 for 24 hours prior to being fixed for 10 minutes using 10% formalin and then permeabilized for 5 minutes using 1X TBS + 0.5% Triton-X100. The cells were incubated with anti-ABCA1 at 5.0ug/ml overnight at 4C and detected with an anti-rabbit Dylight 488 (Green) at a 1:500 dilution. Alpha tubulin (DM1A) NB100-690 was used as a co-stain at a 1:1000 dilution and detected with an anti-mouse Dylight 550 (Red) at a 1:500 dilution. Nuclei were counterstained with DAPI (Blue). Cells were imaged using a 40X objective.



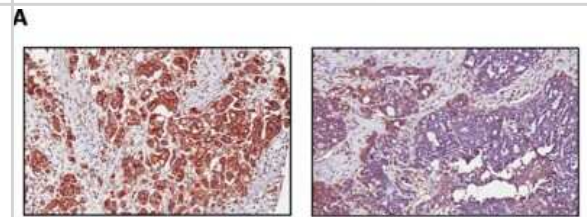
Untreated HepG2 cells were grown to 60% confluency, and serum starved for 24 hours prior to being fixed for 10 minutes using 10% formalin and then permeabilized for 5 minutes using 1X TBS + 0.5% Triton-X100. The cells were incubated with anti-ABCA1 at 5.0ug/ml overnight at 4C and detected with an anti-rabbit Dylight 488 (Green) at a 1:500 dilution. Alpha tubulin (DM1A) NB100-690 was used as a co-stain at a 1:1000 dilution and detected with an anti-mouse Dylight 550 (Red) at a 1:500 dilution. Nuclei were counterstained with DAPI (Blue). Cells were imaged using a 40X objective.



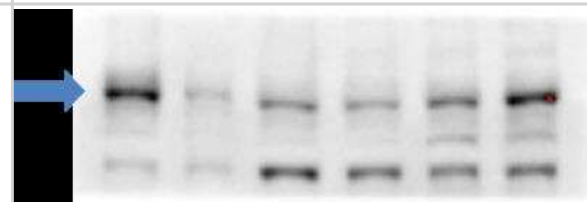
ABCA-1 FITC conjugated antibody of human adipose tissue macrophage subsets by flow cytometry. Image from verified customer review.



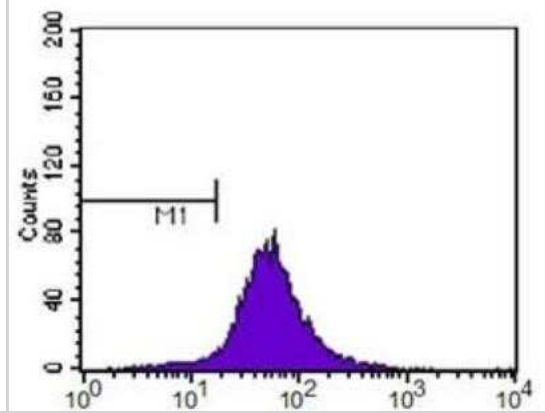
Association between expression of ABCA1 and survival in ovarian cancer patients. Expression of ABCA1 in 55 ovarian cancer patient samples was determined by IHC in tissue microarray. Representative image of ovarian cancer showing high (left panel) and low (right panel) ABCA1 expression on the cell membrane or cytoplasm (x400). Image collected and cropped by CiteAb from the following publication (<https://www.clinicalepigeneticsjournal.com/content/7/1/1>), licensed under a CC-BY license.



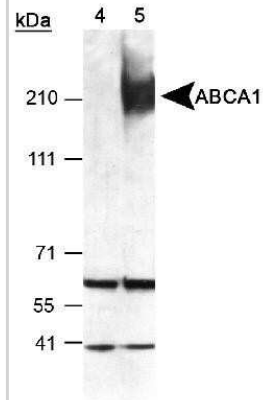
ABCA1 in human primary fibroblasts in culture. 10 ug of total protein. 7.5% TGX gel. Blocking 5% milk in PBST 1h RT. 1:1000 primary ab in BSA 3% PBST O/N at 4C. Secondary 1:5000 HRP 1h RT. Arrow shows around 250 kDa. WB image submitted by a verified customer review.



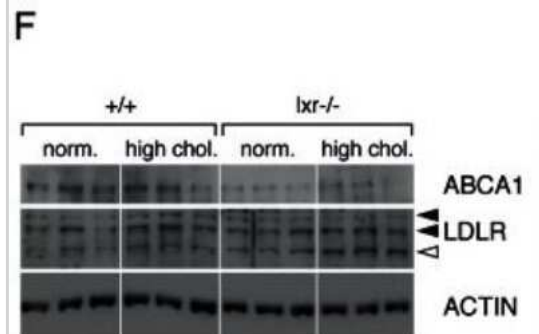
ABCA1 antibody was tested at 1: 400 in HeLa cells using an Alexa Fluor 488 secondary (shown in purple). M1 is defined by unstained cells.



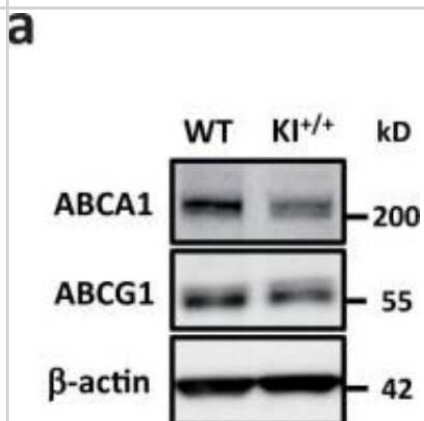
Detection of ABCA1 in mouse peritoneal macrophages using NB 400-105 (Lot L). ECL exposure, 1 min. Lane 4: T09 uninduced lysate Lane 5: T09 induced lysate.



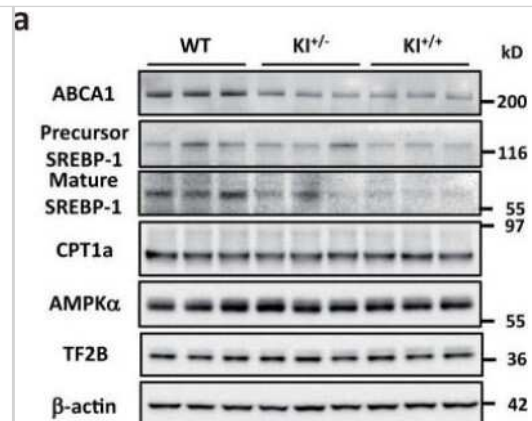
Prostates of LXR mutant mice accumulate cholesterol esters through inappropriate LXR target genes regulation. Total protein lysates of WT and LXR null mice under normal or high cholesterol diet were analyzed by western blotting with antibodies against ABCA1, LDLR and ACTIN as a loading control (left panel), quantification of ABCA1 and LDLR protein accumulation levels (right panel). * $p < 0.05$, *** $p < 0.001$ in Student's t test. Error bars represent the \pm mean SEM. Image collected and cropped by CiteAb from the following publication (<https://dx.plos.org/10.1371/journal.pgen.1003483>), licensed under a CC-BY license.



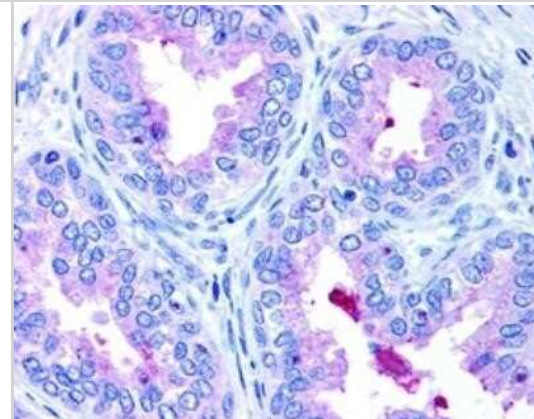
miR-33b reduces cellular cholesterol efflux and serum HDL-C levels. Western blotting for ABCA1 (using NB400-105) and ABCG1 proteins in peritoneal macrophages from WT and KI^{+/+} mice. Representative images are shown. beta-actin was used as the loading control. Image collected and cropped by CiteAb from the following publication (<https://www.nature.com/articles/srep05312>), licensed under a CC-BY license.



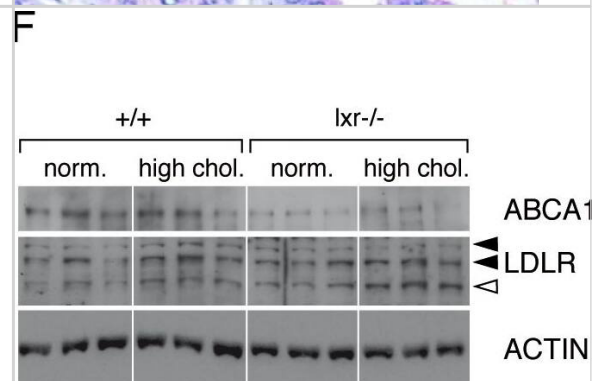
miR-33b regulates ABCA1 and SREBP-1. Analysis for ABCA1, SREBP-1, CPT1a, and AMPK alpha protein levels in the livers of WT, KI^{-/-}, and KI^{+/+} mice. Representative images are shown. TF2B and beta-actin were used as loading controls. Image collected and cropped by CiteAb from the following publication (<https://www.nature.com/articles/srep05312>), licensed under a CC-BY license.



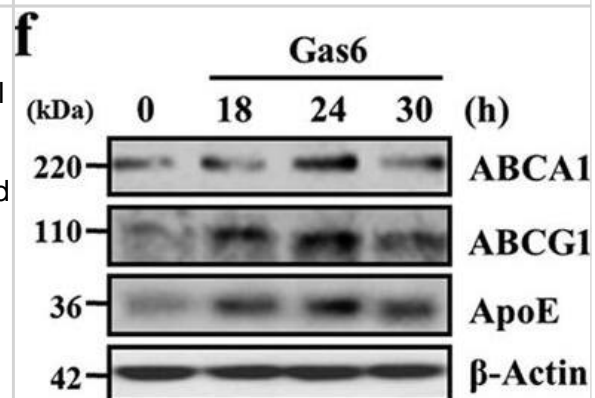
Detection of ABCA1 in human prostate epithelium showing luminal and membrane staining.



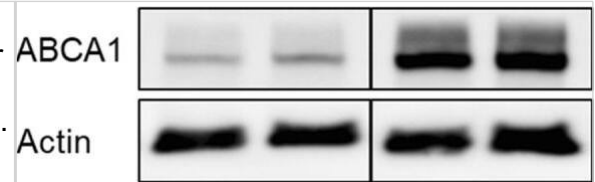
Prostates of LXR mutant mice accumulate cholesterol esters through inappropriate LXR target genes regulation. (A) Plasma concentrations of cholesterol were determined (N = 9/13 per group) after 5 weeks dietary conditional exposure in each genotype. Image collected and cropped by CiteAb from the following publication (<https://pubmed.ncbi.nlm.nih.gov/23675307>), licensed under a CC-BY license.



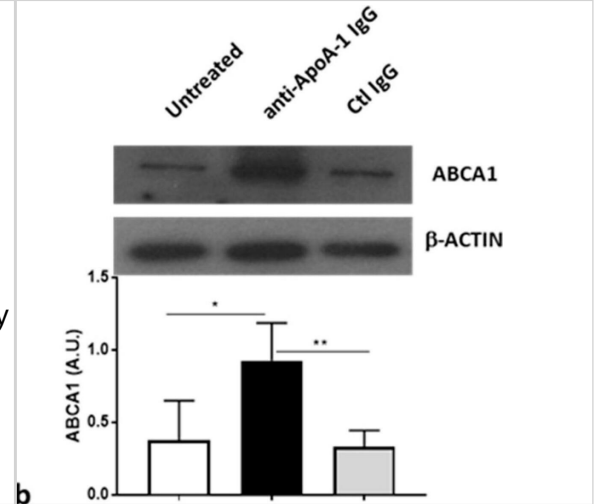
Gas6 treatment enhances expression of LXRalpha and LXRbeta and their target genes in BMDM. Mouse BMDM were stimulated with 400 ng/ml Gas6, 1 uM T0901317, 10 ng/ml interferon (IFN)-gamma, 10 ng/ml IL-4, or 100 ng/ml LPS for 4 h (a,b) or 400 ng/ml Gas6 for the indicated times (c-g). (a,b,e) The amounts of the LXRalpha, LXRbeta, ABCA1, ABCG1, ApoE, AIM, Arg2, VEGF, YM1, and Arg1 mRNAs were analyzed by real-time PCR and normalized to that of Hprt mRNA. (c,d,f,g) The relative abundances of LXRalpha, LXRbeta, ABCA1, ABCG1, ApoE, Aim, Arg2, and VEGF proteins were determined by Western blotting analysis. The relative densitometric intensity was determined for each band and normalized to beta-actin. Data in all bar graphs are means +/- SEM of three independent experiments. *P < 0.05 compared with control. Image collected and cropped by CiteAb from the following publication (<https://pubmed.ncbi.nlm.nih.gov/27406916>), licensed under a CC-BY licence.



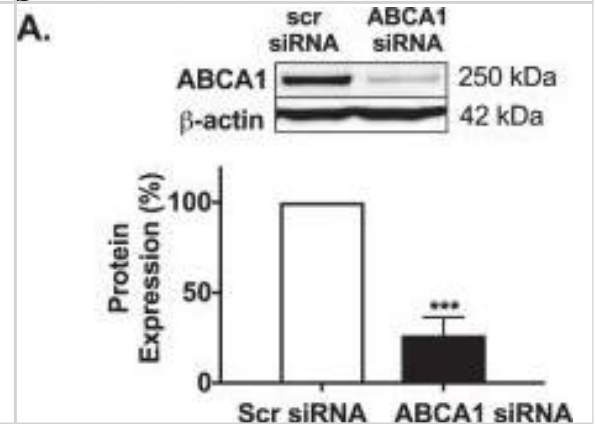
Western Blotting for ABCA1, as detailed in Supplementary Protocol #5 (Additional file 1). Caco-2 cells cultivated on filter inserts were treated for 48 h with bexarotene (RXR agonist, 5 μ M), T0901317 (LXR agonist, 10 μ M), GW3965 (LXR agonist, 10 μ M) or the vehicle control (DMSO 0.1%). Protein expression was then determined by western blot analysis. Results were normalized for interexperimental variance and then set in relation to the vehicle control. Bar graphs represent mean \pm SD from three independent experiments. A representative blot is shown - the bands stem from the same membrane and the vertical line indicates excised irrelevant bands. ns not significant, *P < 0.05, **P < 0.01 versus solvent vehicle (determined by paired t-test) Image collected and cropped by CiteAb from the following publication (<https://pubmed.ncbi.nlm.nih.gov/32308567>), licensed under a CC-BY licence.



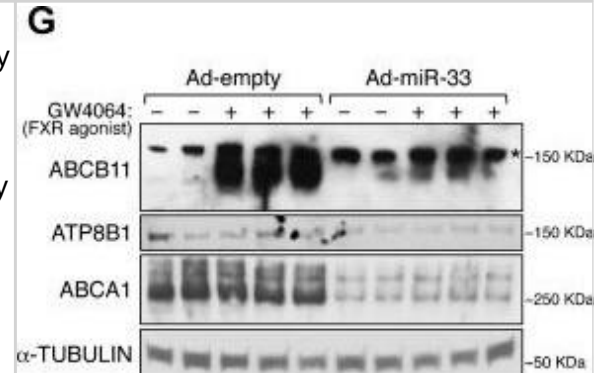
Anti-ApoA-1 IgGs upregulate ABCA1. ABCA1 was increased after 16 and 24 h of anti-ApoA-1 IgG exposure to HMDM at the mRNA level as revealed by RT-PCR (a) as well as at the protein level after 24 h anti-apoA-1 IgG stimulation, as revealed by Western blot analysis (b). In panel a, data are expressed as fold change expression of the mean \pm SD of ABCA1 calculated by $\Delta\Delta$ CT method of six independent experiments (n = 6) and values were normalized to untreated condition. p-values were calculated using the Student's t-test: * p < 0.05, ** p < 0.01, **** p < 0.0001. (b) One of four representative Western blots is shown. Data are the mean \pm SD of band intensity volume/actin intensity volume of four independent experiments (n = 4). p-values were calculated using the Student's t-test: * p = 0.02, ** p = 0.005. Image collected and cropped by CiteAb from the following publication (<https://pubmed.ncbi.nlm.nih.gov/31766415>), licensed under a CC-BY licence.



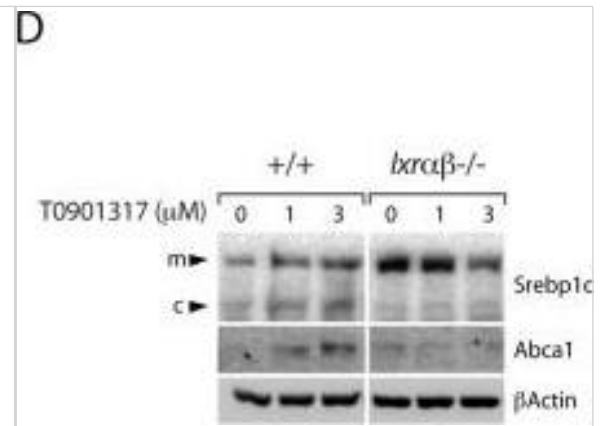
ApoA-I increases glucose uptake in HSKMCs in an ABCA1- and SR-B1-dependent manner. HSKMCs were transfected with scrambled siRNA (scr siRNA), ABCA1 siRNA or SR-B1 siRNA. The cells were lysed and ABCA1 (A) and SR-B1 (B) protein levels were quantified by immunoblotting. Image collected and cropped by CiteAb from the following publication (<https://pubmed.ncbi.nlm.nih.gov/30718702>), licensed under a CC-BY licence.



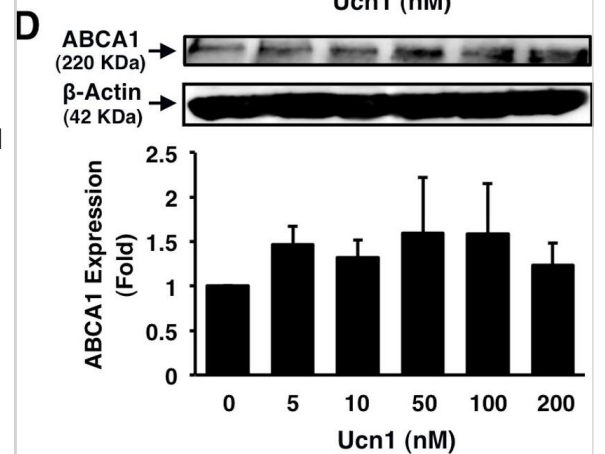
Functional miR-33 responsive elements in the 3'UTR of ATP8B1 and ABCB11. G). Relative protein levels in HuH7 cells transduced with empty or miR-33 adenovirus. Some cells were incubated for 16 h in the presence of FXR:RXR agonists (2 μ mol/L GW4064 : 1 μ mol/L 9-cis-retinoic acid) to induce ABCB11. Asterisk indicates a non-specific band. Data shown as mean \pm SD; **p < 0.01. Image collected and cropped by CiteAb from the following publication (<https://pubmed.ncbi.nlm.nih.gov/22767443>), licensed under a CC-BY licence.



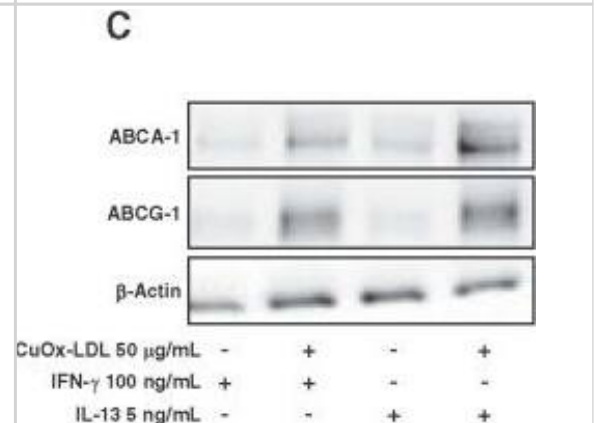
LXRs control expression of genes involved in cholesterol homeostasis and fatty acid synthesis in MPECs. (D) Western blot analysis was performed on WT (+/+) or *Lxralphabeta*^{-/-} MPECs using Srebp1c, Abca1 and beta-Actin antibodies. Image collected and cropped by CiteAb from the following publication (<https://pubmed.ncbi.nlm.nih.gov/23554947>), licensed under a CC-BY licence.



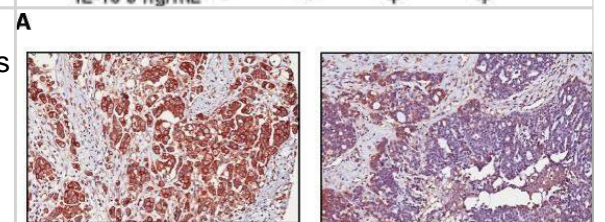
Suppressive effects of Ucn1 on foam cell formation and related protein expression in human monocyte-derived macrophages. Human monocytes were incubated for 7 days with RPMI-1640 supplemented with 10% human serum and the indicated concentrations of Ucn1, followed by a 19 h-incubation with 50 μg/ml oxLDL in the presence of 0.1 mmol/l [³H]oleate. Intracellular CE accumulation was determined from the radioactivity of cholesterol-[³H]oleate. Otherwise, before the addition of oxLDL, cells were harvested and subjected to immunoblotting analyses for CD36, ACAT1, or ABCA1. beta-Actin served as a loading control. Data are expressed as means ± SEM from 4-6 independent experiments with monocytes from 4-6 different donors. Baseline (1 fold) = 8.4 ± 2.2 nmol/mg cell protein. *P < 0.05, +P < 0.001 vs. 0 nmol/l of Ucn1. Image collected and cropped by CiteAb from the following publication (<https://dx.plos.org/10.1371/journal.pone.0110866>), licensed under a CC-BY licence.



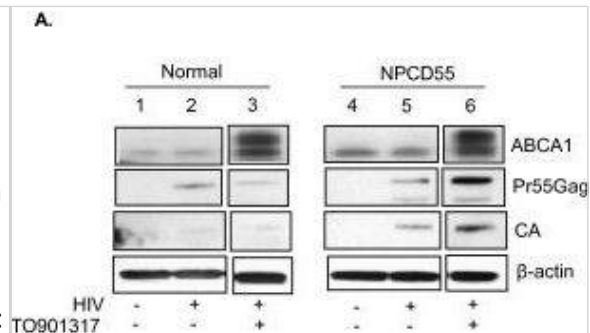
Alternatively activated macrophages (M2) exhibit increased clearance of OxLDL in vitro C). Increased ABCA1 and ABCG1 expression in M2-derived foam cells. Shown is a representative Western blot for the presence of ABCA1, ABCG1 and beta-actin in lysates of cells that were treated as indicated. Image collected and cropped by CiteAb from the following publication (<https://pubmed.ncbi.nlm.nih.gov/23027612>), licensed under a CC-BY licence.



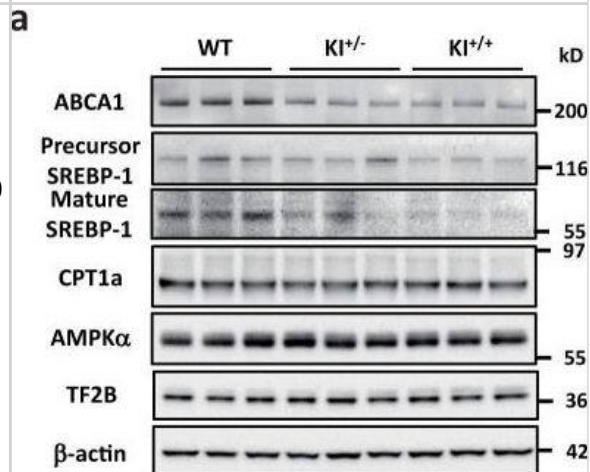
Association between expression of ABCA1 and survival in ovarian cancer patients. Expression of ABCA1 in 55 ovarian cancer patient samples was determined by IHC in tissue microarray. (A) Representative image of ovarian cancer showing high (left panel) and low (right panel) ABCA1 expression on the cell membrane or cytoplasm (x400). Image collected and cropped by CiteAb from the following publication (<https://clinicalepigeneticsjournal.biomedcentral.com/articles/10.1186/s13148-014-0036-2>), licensed under a CC-BY licence.



Impairment of mitophagy upon Antimycin A and Oligomycin exposure. **a** Cells were treated with Antimycin A (1 μ M) and Oligomycin (1 μ M) for 1, 3, and 6 and mitochondrion/cytosol fractionation was performed to assay the accumulation of LC3-II, p62 and PINK1 within the mitochondrial fraction. VDAC1 was used as a loading control for mitochondrial fractions. **b, c** Cells were treated with Antimycin A (1 μ M) and Oligomycin (1 μ M) for 1, 3, 6, and 24 h and total fibroblasts extracts were analyzed for PINK1, p62, COXIV and VDAC1. Each quantitative data was normalized with ACTIN ($n \geq 3$). Statistical analysis was performed using two-way ANOVA with Tukey's multiple comparisons test. (* $p < 0.05$; ** $p < 0.01$; *** $p < 0.001$). Immunoblots reported are from one representative experiment Image collected and cropped by CiteAb from the following open publication (<https://pubmed.ncbi.nlm.nih.gov/31332166>), licensed under a CC-BY license. Not internally tested by Novus Biologicals.

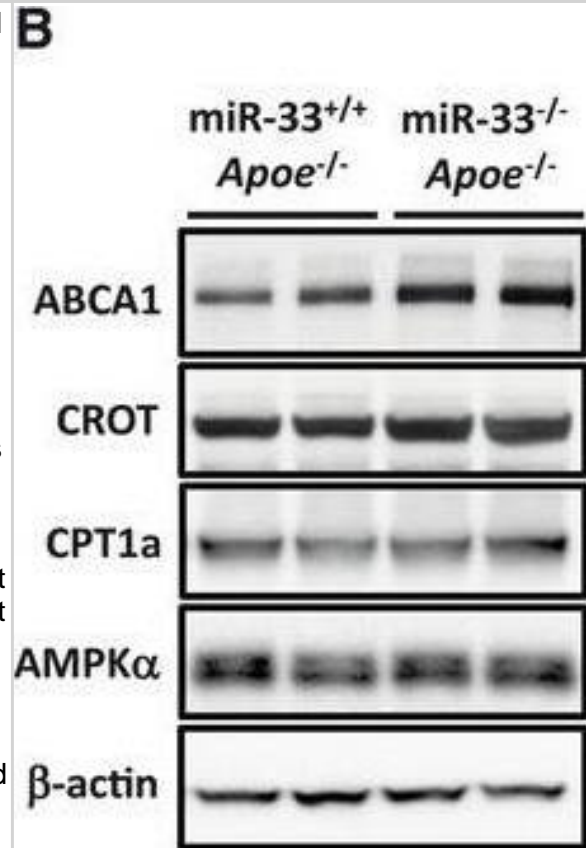
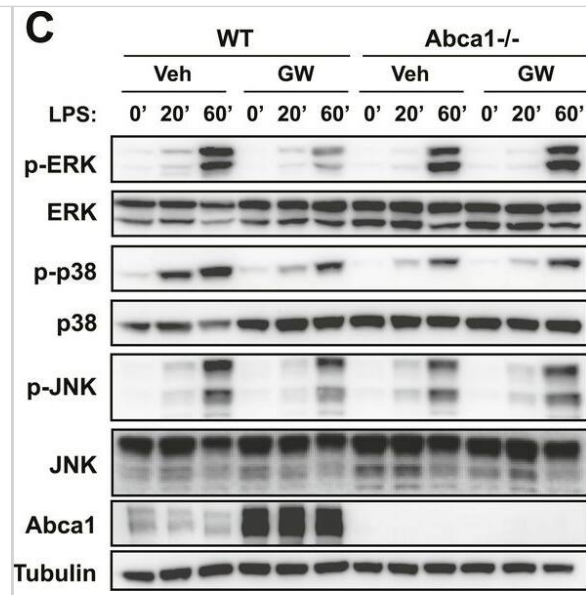


GPR50 competes with FKBP12 for the binding to T β RI. **a** (Left) HEK293T cells were transfected with Flag-T β RI alone or cotransfected with HA-T β RII (with TGF β ; 2 ng/mL; 1 h), myc-FKBP12 and either GPR50 Δ 4 or GPR50wt. Lysates were precipitated for FKBP12 using anti-myc antibody and blotted with an anti-Flag to reveal complex formation. Expression of myc-FKBP12, Flag-T β RI, HA-T β RII and GPR50 was determined in total lysates. (Right) Densitometric analysis of 3 independent experiments (Mean \pm s.e.m., $n = 3$ independent experiments, ** $p < 0.01$, one-way ANOVA with Dunnett's post hoc test). **b, c** Competition between FKBP12 and GPR50 for T β RI binding was checked by precipitating FKBP12 from total brain and lung lysates of wt and GPR50ko mice and revealed with anti-T β RI. Total lysate was addressed for expression of FKBP12, T β RI, and GPR50 with corresponding antibodies. **d** To address the competition of FKBP12 and GPR50 for T β RI binding, BRET measurements were performed with HEK293T cells expressing fixed amounts of T β RI-Rluc8 and GPR50 Δ 4-YFP or GPR50wt-YFP or T β RII-YFP and stimulated with TGF β (0.6 nM, 30 min, 37 $^{\circ}$ C). Immunoblot on the top shows FBP12 expression when transfected either with empty (Mock) or FKBP12 in different conditions. **e** HEK293T cells expressing the indicated proteins were starved and treated for 1 h with 2 ng/ml of TGF β or 100 ng/ml of FK506. Total lysates were immunoblotted for Smad3 phosphorylation and total expression of myc-Smad3, GPR50 and myc-FKBP12 with suitable antibodies. **f** Alignment of FKBP12 and GPR50 sequences revealed similarities between the C-terminal "ATGHP" motif in FKBP12 and four repetitive motifs in GPR50 (upper top panel). One motif of GPR50 is located close to the Δ 4 deletion of GPR50 Δ 4 (lower bottom panel). Structural data with permission adapted from Huse et al.²⁹ highlight the implication of the HP loop (red) in binding to T β RI (lower panel). **g** HEK293T cells were transfected with indicated plasmids and as in **a**. Lysates were precipitated for FKBP12 using an anti-myc antibody and blotted with an anti-T β RI to reveal complex formation. Expression of myc-FKBP12, HA-T β RI, and GPR50 was determined in total lysates. Representative results are shown for **b, c, e, and g**. Similar results were obtained in at least two additional experiments. See also Supplementary Fig. 3 Image collected and cropped by CiteAb from the following open publication (<https://www.nature.com/articles/s41467-018-03609-x>), licensed under a CC-BY license. Not internally tested by Novus Biologicals.

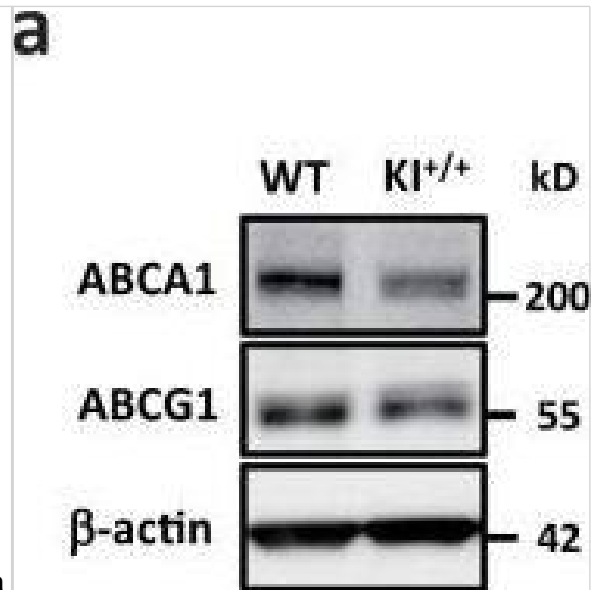


Involvement of CBP in BNIP3 expression regulated by HIF-1 α and FOXO3 under hypoxia. (A) UCB-hMSCs were incubated with hypoxia condition for 24 h. Co-immunoprecipitation of HIF-1 α and FOXO3 with IgG and CBP were shown in left panel. IgG was used as a negative control. The total protein expressions of HIF-1 α , FOXO3, CBP and β -actin in lysate were shown in right panel. $n = 3$. (B) CBP (20 μ M) was pretreated to UCB-hMSCs, and cells were incubated with hypoxia for 24 h. The BNIP3 mRNA expression level was analyzed by qPCR. $n = 6$. (C) BNIP3 and β -actin protein expressions were analyzed by western blot. Data represent mean \pm S.E. $n = 4$. (D, E) Sample DNA was immuno-precipitated with RNA polymerase, IgG, HIF-1 α and FOXO3 specific antibodies. CHIP (top panel) and lysate (bottom panel) samples were amplified with the primers of GAPDH and BNIP3 promoters. Quantitative CHIP data was analyzed by qPCR, and shown in the right panel. $n = 4$. Western blot data were normalized by β -actin, and qPCR data were normalized by ACTB mRNA expression level. Quantitative data are presented as a mean \pm S.E.M. All blot images are representative. * $p < 0.05$ versus control, # $p < 0.05$ versus hypoxia. Image collected and cropped by CiteAb from the following open publication (<https://linkinghub.elsevier.com/retrieve/pii/S2213231717303804>), licensed under a CC-BY license. Not internally tested by Novus Biologicals.

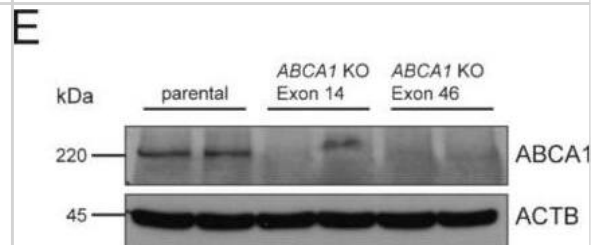
DNA methylation and expression level of the PHD3 gene in HCT116 and DLD-1 CRC cells. A. HCT116 and DLD-1 cells were cultured under normoxic or hypoxic (1% O₂) conditions for 48 hrs. Cells were then used for DNA isolation followed by bisulfite modification. Methylation percentage of three DNA fragments within the PHD3 CpG island (Additional file 1, Additional file 2) in HCT116 and DLD-1 cells under hypoxic and normoxic conditions was determined by Real Time PCR amplification of bisulfite treated standard and cell line DNA, followed by comparison of their HRM profiles. B. Cells were cultured in DMEM either in hypoxic (1%O₂) or normoxic conditions for 48 hrs. After incubation, the cells were used for total RNA isolation and reverse transcription. The PHD3 cDNA levels were determined by RQ-PCR relative quantification analysis. RQ-PCR results were standardized by the geometric mean of PBGD and hMRPL19 cDNA levels. PHD3 cDNA levels are expressed as a multiplicity of these cDNA copies in the cell line's calibrator. C. Cells were cultured in DMEM either in hypoxic (1%O₂) (H) or normoxic (N) conditions for 48 hrs. Cells were then used for protein isolation. Proteins were separated by 10% SDS-PAGE, and transferred to a membrane that was then immunoblotted with Rp anti - PHD3 Ab and incubated with goat anti-rabbit HRP-conjugated Ab. The membrane was then stripped and reblotted with Rp anti-GAPDH Ab, followed by incubation with goat anti-rabbit HRP-conjugated Ab. The band densitometry readings were normalized to GAPDH loading control. The ratio of PHD3 to GAPDH for DLD-1 in normoxic conditions was assumed to be 1. Image collected and cropped by CiteAb from the following open publication (<https://pubmed.ncbi.nlm.nih.gov/24195777>), licensed under a CC-BY license. Not internally tested by Novus Biologicals.



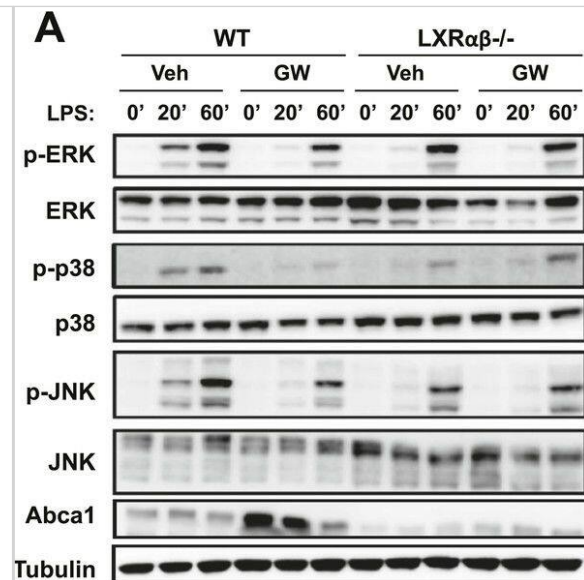
The role of HIF-1 in purinosome formation. a, quantifying the number of purinosome-containing cells in normoxia or hypoxia (24 h) in purine-rich medium and normoxia in purine-depleted medium (purine -ve), cells in hypoxia transfected with siRNA to HIF-1 α (+ siRNA), and cells in purine-rich medium supplemented with DFX. Data shown are n = 3, mean \pm S.E., total number of cells counted are shown in parentheses. b, time course of purinosome formation in hypoxia shows the number of purinosome-containing cells steadily increases after 3 h in hypoxia. Re-oxygenation of the samples after hypoxic incubation for 10 h reverts the number purinosome-containing cells back to normoxic levels. Data shown is n = 3, mean \pm S.E., total number of cells counted are shown in parentheses. c, time course of HIF-1 α stabilization in hypoxia shows maximum HIF-1 α protein expression levels at 3 h in hypoxia, after which the HIF-1 α expression decreases. The positions of molecular markers are shown for each blot; uncropped blots with overlaid markers are deposited in the raw data files. d, the effect of hypoxia on the transcription of purine biosynthesis enzymes measured by qPCR. Vascular endothelial growth factor (VEGF) and HIF-1 α are controls. Data shown are n = 5, mean \pm S.E. e, the effect of hypoxia on the protein expression levels of the purine biosynthetic enzymes. HIF-1 α is stabilized in hypoxia as expected, and no significant increase in the purine enzymes was detected between normoxic (21% oxygen) and hypoxic (1% oxygen) growth conditions. The positions of molecular markers surrounding each band of interest are shown for each blot; uncropped blots with overlaid markers are deposited in the raw data files. Image collected and cropped by CiteAb from the following open publication (<https://pubmed.ncbi.nlm.nih.gov/32439803>), licensed under a CC-BY license. Not internally tested by Novus Biologicals.



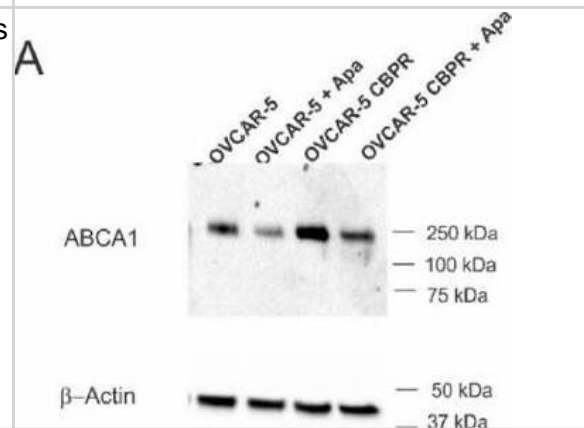
FIH exits the nucleus via a Leptomycin B-sensitive exportin1-dependent pathway. (A) Immunofluorescence staining of FIH (green) and HIF1 α (red) in MCF7 cells after the indicated hypoxia (0.5% O₂) and re-oxygenation treatments. TO-PRO-3 (blue) was used to stain nuclei. (B) Total cell lysates from U2OS cells were immunoprecipitated with an anti-exportin1 antibody or control IgG. FIH, exportin1 and β -tubulin levels are indicated. (C) Immunofluorescence staining of FIH (green) in FIH-null mouse embryonic fibroblasts (MEFs) transfected with HA-FIH 1–349 or HA-FIH Δ NES followed by normoxia, hypoxia (1% O₂, 3 h) or 3 h of hypoxia followed by re-oxygenation for 1 h. TO-PRO-3 (blue) was used to stain nuclei. Arrows indicate nuclear localization of signal. (D) Total cell lysates from U2OS cells transfected with control vector, HA-FIH 1–349 or HA-FIH Δ NES were immunoprecipitated with an anti-exportin 1 antibody. HA-FIH, exportin1 and β -tubulin levels are indicated. FL, full length; IgGL, IgG light chain. Scale bars: 20 μ m. Image collected and cropped by CiteAb from the following open publication (<https://pubmed.ncbi.nlm.nih.gov/30333145>), licensed under a CC-BY license. Not internally tested by Novus Biologicals.



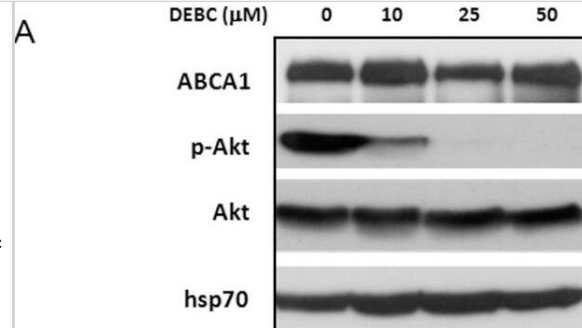
Munc13-4 KD strongly impairs exosome release. (A) SDS-PAGE Western blot of indicated proteins in MDA-MB-231 cells after stable expression of shRNA for Munc13-4 or Rab27a or a scrambled control (Ctrl). (B) Culture medium from MDA-MB-231 cells either untreated or stimulated with 1.25 μ M ionomycin for 30 min was centrifuged at 1,000 g to remove cellular debris and 10,000 g to remove large extracellular vesicles. (C) The resulting 10,000-g supernatant was filtered onto a nitrocellulose membrane and analyzed for CD63, CD9, ALIX, and GM130 content by antibody blotting. (D) Quantification of CD63, CD9, and ALIX blots in C are shown as exosome release as a percentage of total cellular material with mean values \pm standard error (SE) for $n \geq 3$. *, $P < 0.05$ for comparison with corresponding control samples. (E) Panc-1 or A549 cells were left untreated or were treated with TGF β -1 for 24 h. Indicated proteins were detected by SDS-PAGE Western blot. (F) Panc-1 cells were left untreated or were treated with TGF β -1 for 24 h, and Munc13-4 levels were determined by immunofluorescence. TGF β -1-treated cells exhibited a mesenchymal morphology. Bars, 5 μ m. (G) A549 cells stably expressing control shRNA (Ctrl) or Munc13-4 shRNA were left untreated (Untr) or were treated with TGF β -1 for 24 h, and SDS-PAGE Western blotting for indicated proteins was conducted. (H) Culture media supernatants (as in B) from A549 cells that were either untreated or were stimulated with 1.25 μ M ionomycin for 30 min were filtered onto nitrocellulose membrane and analyzed for CD63 and GM130. (I) Quantification of CD63+ exosome release shown as a percentage of total cellular material with mean values \pm SE for $n = 5$. *, $P < 0.05$; **, $P < 0.01$ for comparison with corresponding control samples. Image collected and cropped by CiteAb from the following open publication (<https://pubmed.ncbi.nlm.nih.gov/29930202>), licensed under a CC-BY license. Not internally tested by Novus Biologicals.



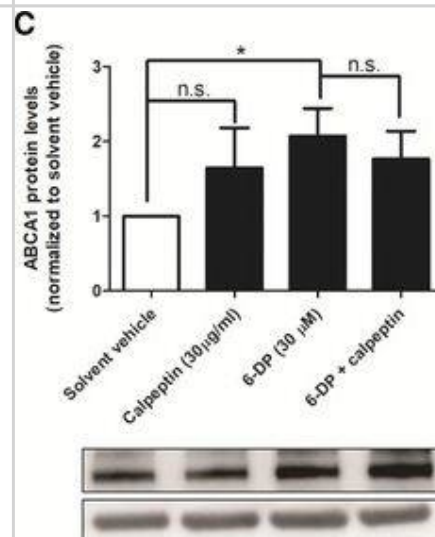
Elevated Spy1 levels prevent contact inhibition. (A) Representative views of focus formation assays in NIH3T3 cells transfected with Myc-Spy1-WT, Myc-Spy1-TST, positive control Ras-V12 or empty vector PCS3 control. $n = 3$ (B) Quantification of the number of colonies. Error bars reflect SE between triplicate experiments. t test was performed; ** $P \leq 0.01$. $n = 3$ (right panel) Western blot analysis of one representative lysate from A-B. Image collected and cropped by CiteAb from the following open publication (<https://bmccancer.biomedcentral.com/articles/10.1186/1471-2407-12-45>), licensed under a CC-BY license. Not internally tested by Novus Biologicals.



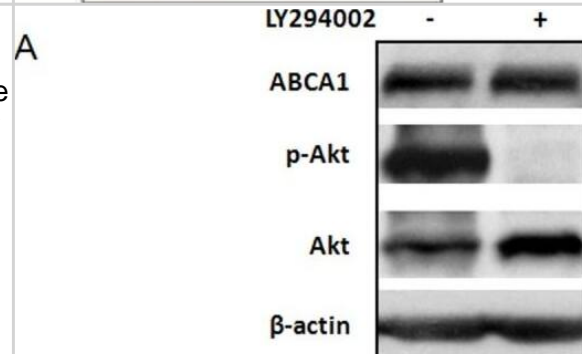
SOD2 mRNA and protein expression. RT-PCR: (A) SOD2 mRNA expression is higher in adults, and highest in the adult parenchyma. (B) No exposure effects on SOD2 mRNA were observed in neonates. (C) Adult SOD2 mRNA was decreased in PFP48. Data are presented as mean+SEM (n=5-7 rats/group, in each compartment), * significantly different compared to neonates in the same compartment, † significantly different compared to airways in the same age, ‡ significantly different compared to FA in the same compartment. Western blotting: (D) Scan of representative SOD2 and actin blots. (E) Neonatal whole lung SOD2 protein expression was unchanged with exposure, and (F) adult whole lung SOD2 protein trended upwards at PFP2, but was statistically insignificant. (G-J) Immunohistochemical localization of SOD2 in lung (n=6 rats/group). SOD2 protein was more abundant in adults compared to neonates, but no exposure specific differences were observed. Scale bar is 50 μ m. Image collected and cropped by CiteAb from the following open publication (<https://particleandfibretotoxicology.biomedcentral.com/articles/10.1186/1743-8977-10-34>), licensed under a CC-BY license. Not internally tested by Novus Biologicals.



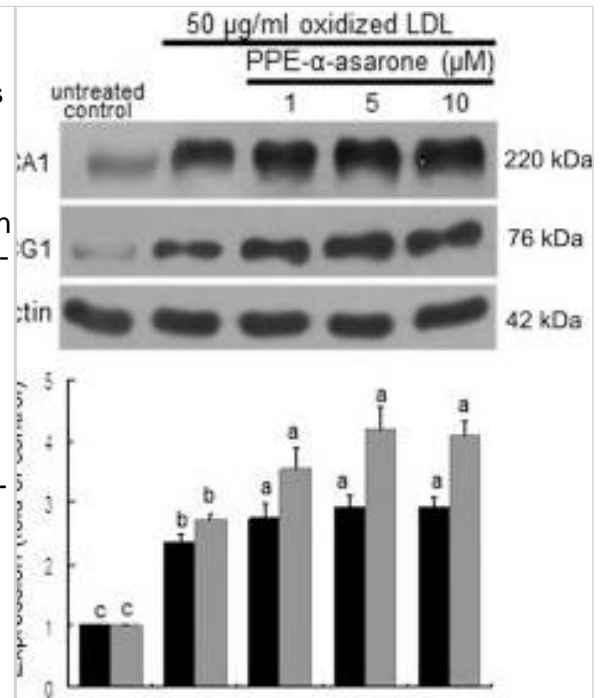
Cells of human meninges co-express LLEC markers. a–c DAB-IHC with single antibodies detects VEGFR3 (a), LYVE1 (b), and MRC1 (c) in the meninges of human post mortem brain showing no signs of neuropathology. These images are taken from a 38 year old male (sample P17/07, Table 1), and confirmed in n = 2 additional samples. P parenchyma. Scale = 150 μ m (a); 40 μ m (b); and 20 μ m (c). d–f DAB-IHC with single antibodies detects VEGFR3 (b), LYVE1 (c), and MRC1 (d) in elderly human meninges (age: 89–92) with evidence of neuropathology and confirmed in n = 3 brains (Table 1). P, parenchyma. Scale = 20 μ m. g–p IHC with fluorescent antibodies detects human meningeal cells that co-express MRC1 (h, m, yellow), LYVE1 (i, n, white), and VEGFR3 (j, o, green). Nuclei/RNA are labelled with DAPI (g, l, blue) and images are merged in (k, p). Scale = 10 μ m Image collected and cropped by CiteAb from the following open publication (<https://pubmed.ncbi.nlm.nih.gov/31696318>), licensed under a CC-BY license. Not internally tested by Novus Biologicals.



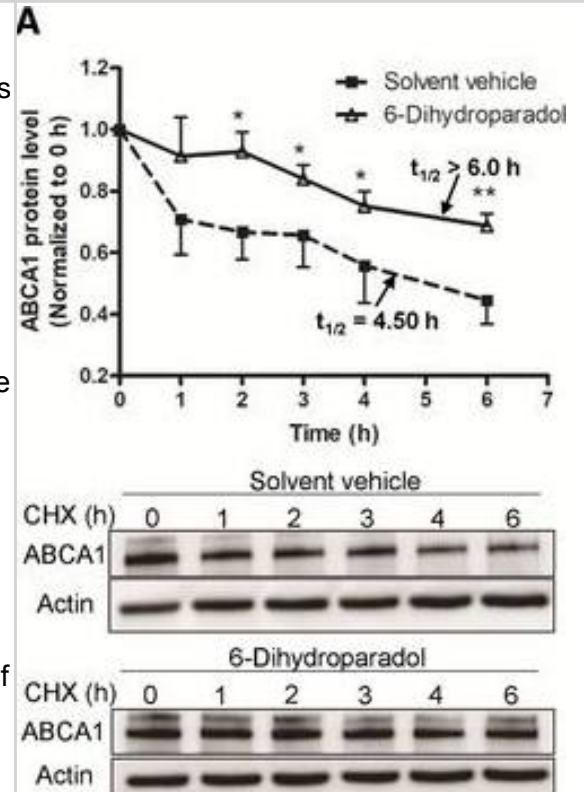
Inhibition of KDM expression in vivo. (A) Ears from C57Bl/6 mice were injected intradermally with 250 ng of IL-1 α , IL-17A, IL-22, OSM and TNF α (M5) or with Phosphate Buffered Saline (PBS). At 24 h quantitative RT-PCR analysis was carried out on total RNA and expression levels for cytokeratin 1 (CK1), cytokeratin 10 (CK10), loricrin (LOR), filaggrin (FLG), desmoglein 1 (DSG1), desmocollin 1 (DSC1) and involucrin (IVL) were normalized using GAPDH housekeeping gene and expressed as the fold decrease under non injected skin. Data are represented as mean and SEM of 3 independent experiments. *p<0.05, **p<0.01, ***p<0.001. (B) On day 2, the ears were collected for staining with Hematoxylin and Eosin (HE) and immunodetection of cytokeratin 10, loricrin, filaggrin, cytokeratin 6 and Ki-67. Scale bar 100 μ m. Results are from one experiment representative of three. (C) Skin biopsies from normal control skin (Cont) or lesional psoriatic skin (Pso) were collected. Skin sections were stained with Hematoxylin and immunodetection of cytokeratin 10, loricrin, filaggrin, involucrin and S100A7 was performed. Scale bar 100 μ m. Results are from one experiment representative of three. Image collected and cropped by CiteAb from the following open publication (<https://dx.plos.org/10.1371/journal.pone.0101937>), licensed under a CC-BY license. Not internally tested by Novus Biologicals.



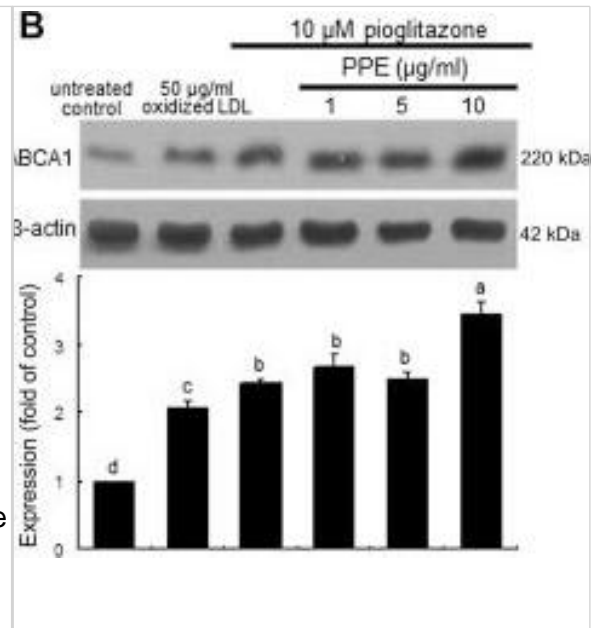
MicroRNA-214-3p (miR-214) mimic in rat vascular smooth muscle cells (A7r5) suppressed angiogenesis and proliferation but promoted senescence. a Schematic of the protocol for transfection of A7r5 VSMCs with a miRNA mimic control (mimic NC) or a miR-214 mimic and processed at the indicated times. b The effects of miR-214 mimic on VSMC cell proliferation were tested by CCK-8 assay. c Angiogenic mRNA expressions of NOS3, VEGFA, CXCL12 and CXCR4 compared in cells transfected with mimic NC or miR-214 mimic (n = 3). d Senescence-associated mRNA expressions of TERT, TERF1 and TERF2 compared in cells transfected with mimic NC or miR-214 mimic (n = 3). e, g Representative western blots depicting TERF1, TERF2, p16INK4, p21CIP1, pRB, and quaking expression in mimic NC or miR-214 mimic transfected cells. f, h Normalized expressions of TERF1, TERF2, p16INK4, p21CIP1, pRB, and quaking (n = 3). i Senescence-associated β -galactosidase staining demonstrating senescence in mimic NC or miR-214 mimic transfected cells. j Bar graphs show quantification of relative of SA- β -gal positive cells (n = 3). Data are presented as the means \pm SEM. * P < 0.05; ** P < 0.01; *** P < 0.001 (Two-tailed Student's t-test) Image collected and cropped by CiteAb from the following open publication (<https://pubmed.ncbi.nlm.nih.gov/32410577>), licensed under a CC-BY license. Not internally tested by Novus Biologicals.



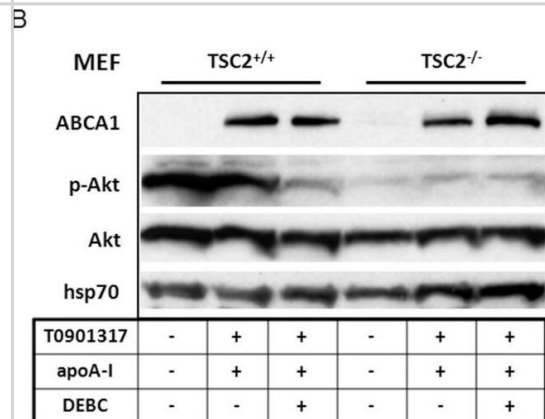
Intraperitoneally Administered Compound A Effectively Suppresses Triple-Negative Breast and Blood Cancer Xenograft Tumor Growth. Immunocompromised mice were subcutaneously injected with cancerous cell lines and tumors were allowed to establish. Treatments occurred every other day and the studied compound or the equivalent vehicle control administered intraperitoneally for five weeks. Tumor volume and mass were measured two times per week. (a) MV-4-11 xenograft study was administered with approximately 5.0 mg/kg of Compound A and 5.0 mg/kg of curcumin. Results are representative for the Control (n = 5), Compound A (n = 5), and curcumin (n = 4) treated group, each with two tumors per mouse. (b) MDA-MB-231 xenograft study was administered with approximately 7.5 mg/kg of Compound A. Results are representative for the Control (n = 3) and Compound A (n = 4), each with one tumor per mouse. Scale bar is 1 centimeter. (c) Immunohistochemistry analysis of sectioned tumor tissues from the MDA-MB-231 study. Each section was subjected to the specified antibody followed by a biotinylated secondary antibody. Detection was done using a DAB Peroxidase HRP Substrate Kit (brown) followed by Hematoxylin counterstaining (purple). Images were obtained using inverted bright field microscopy. Sectioning results are representative of three individual tumors. Scale bar is 50 microns. Statistical analysis using One-Way ANOVA. *p < 0.05 vs tumor volume of the control. Image collected and cropped by CiteAb from the following open publication (<https://pubmed.ncbi.nlm.nih.gov/28439094>), licensed under a CC-BY license. Not internally tested by Novus Biologicals.



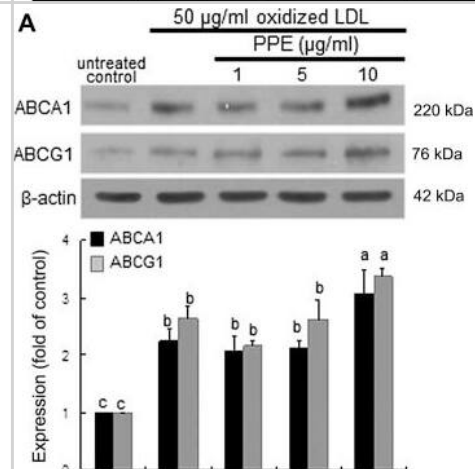
Mechanical tensile strain of 30% induces an elongation of paranodal junction and alteration in MAPK signaling in organotypic cerebellar slice culture. a Double immunostaining of organotypic cerebellar slices for CASPR in red and MAG in green. The response was evaluated at time 0 h post-stretch. Altered paranodal junctions are highlighted within white circles in high-magnification images. Scale bar, 50 μ m; inset scale bar, 5 μ m. b Sketch of CASPR and MAG labeling in the paranodal junction. Quantitative analysis is characterized by three length measurements: c nodal length called (A); d paranodal length called (B); and e (B-A) corresponding to the total length of the CASPR labeling. f-h Proteins were extracted following strain of 30% from control (Ctrl) and stretched (Stretch) slices and western blot was performed for the myelin protein MBP (f), ERK1/2 (g), and p38 (h). The ratio P-ERK on total ERK and the ratio P-p38 on total p38 are presented. β -Actin was used as a loading control. Results represent the mean \pm SEM (n = 3). ***p < 0.001. CASPR contactin-associated protein, MAG myelin-associated glycoprotein Image collected and cropped by CiteAb from the following open publication (<https://pubmed.ncbi.nlm.nih.gov/30298339>), licensed under a CC-BY license. Not internally tested by Novus Biologicals.



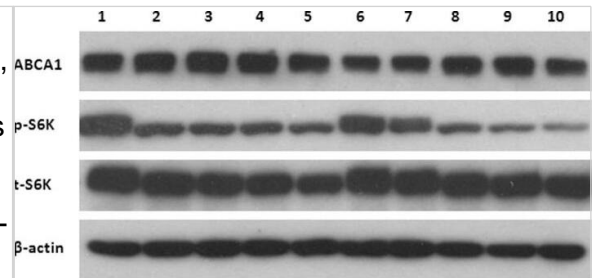
Gomisin N (GN) represses the expression of JMJD2B, PPAR γ 2, and PPAR γ 2 steatosis target genes in HepG2 cells. HepG2 cells were treated with GN (100 μ M) for 12 h. (A) JMJD2B expression was assessed by qPCR and western blotting. The full-length western blots corresponding to truncated blots are given in Supplementary Figure S4. (B) PPAR γ 2 expression was measured by qPCR. (C,D) The expression of PPAR γ 2 steatosis target genes was assessed by qPCR. Data represent means \pm SEM of three independent experiments performed in triplicate. *p < 0.05 vs. no treatment. Image collected and cropped by CiteAb from the following open publication (<https://pubmed.ncbi.nlm.nih.gov/30214048>), licensed under a CC-BY license. Not internally tested by Novus Biologicals.



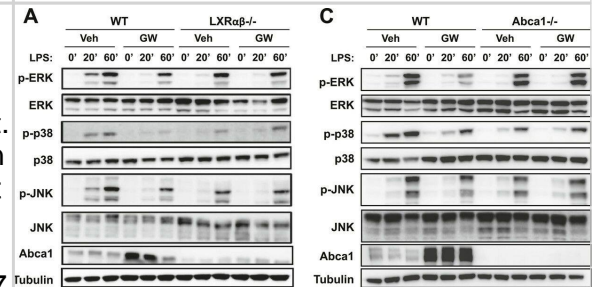
TCAB1 knockdown inhibits tumor growth in vivo. a. shTCAB1-C and shScra cells were injected subcutaneously into the left and right neck of the nude mice respectively. Measured the tumors size from the 11th day using vernier caliper and calculated the volume of tumors by formula $l*w*h/2$ (mm³). Finally, got out the xenografts carefully after mercifully killed the mice. b. Measured the final volume and weighted the final weight of the removed tumors. c. Performed IHC against TCAB1 using mice xenografts sections. The smaller tumors expressed less TCAB1 compared to shScra cells. Statistical analysis of the IHC data used Aperio ImageScope software and all of the data were determined by Student's t test (*P < 0.05, **P < 0.01, ***P < 0.005). Image collected and cropped by CiteAb from the following open publication (<https://pubmed.ncbi.nlm.nih.gov/25070141>), licensed under a CC-BY license. Not internally tested by Novus Biologicals.



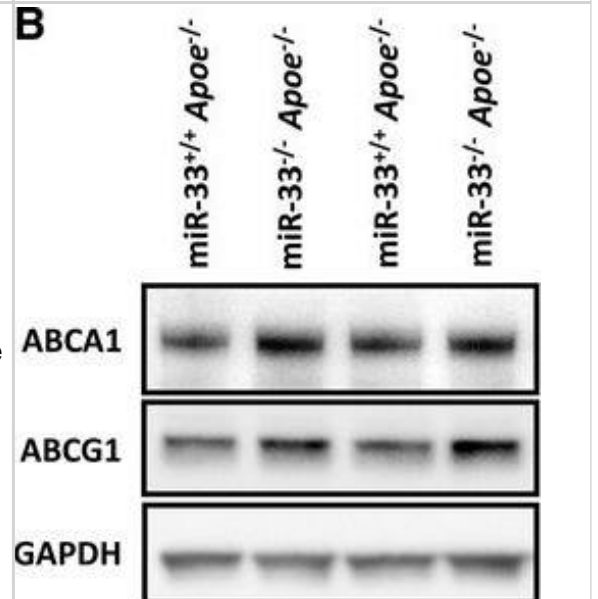
MiR-375-3p negatively regulates Derlin-1 and blocks EMT in BFTC909 cells. (A) Western blot revealed the restoration of Derlin-1, MMP-2, Snail, and ZEB1 after co-transfection of miR-375-3p mimics and CMV-Derlin-1 compared with cells transfected with miR-375-3p alone in BFTC909 cells with α -tubulin as a reference (B) Quantification of the protein levels of Derlin-1, occludin, MMP-2, Snail, and ZEB1 from (A) (N = 3). (C) miR-375-3p suppressed BFTC909 cell migration ability but restored by Derlin-1 overexpression (N = 3). (D) miR-375-3p repressed invasion of BFTC909 cells but restored by Derlin-1 overexpression (N = 3). Data were represented as mean \pm SD; * $p < 0.05$, ** $p < 0.01$. Image collected and cropped by CiteAb from the following open publication (<https://pubmed.ncbi.nlm.nih.gov/35205628>), licensed under a CC-BY license. Not internally tested by Novus Biologicals.



JMJD2B expression increases in hepatic steatotic cell and animal models. (A) HepG2 cells were incubated with a mixture of palmitic acid (PA) and oleic acid (OA) (1:2 ratio) at 800 μ M concentrations for 24 h, and intracellular triglyceride (TG) levels were analyzed by a TG assay kit. JMJD2B mRNA and protein levels were examined by qPCR and western blotting, respectively. Data represent means \pm SEM of three independent experiments performed in triplicate. * $p < 0.05$ vs. no treatment. The full-length western blots corresponding to truncated blots are presented in Supplementary Figure S1A. (B) HepG2 cells were treated with T0901317 (10 μ M) for 24 h, and intracellular triglyceride (TG) levels were measured by a TG assay kit. JMJD2B mRNA and protein levels were examined by qPCR and western blotting, respectively. Data represent means \pm SEM of three independent experiments performed in triplicate. * $p < 0.05$ vs. no treatment. The full-length western blots are presented in Supplementary Figure S1B. (C) Total RNAs were isolated from the livers of HFD-induced obese mice. The JMJD2B mRNA levels were assessed by qPCR. Data represent means \pm SEM of 5 mice. * $p < 0.05$ vs. ND mice. ND: normal diet. HFD: high fat diet. Image collected and cropped by CiteAb from the following open publication (<https://pubmed.ncbi.nlm.nih.gov/30214048>), licensed under a CC-BY license. Not internally tested by Novus Biologicals.



TLR4 expression in pVW-MSCs cultured with or without LPS (10 μ g/ml) for 1 and 4 h and after additional 24 h of recovery after LPS removal (4hR). a: flow cytometry analysis were performed in not fixed and not permeabilized cells for TLR4 surface expression determination (TLR4: Surface) and in fixed and permeabilized cells to measure the overall TLR4 amount (TLR4: Total). Red histograms: stained cells; blue histograms: control cells. b: representative Western Blot of TLR4 and housekeeping β -tubulin and relative quantification were presented. c: representative images of TLR4 immunostaining of pVW-MSCs cultured with or without LPS (10 μ g/ml) for 4 h. pVW-MSCs nuclei were stained with Hoechst 33258 (blue). Scale bar = 10 μ m. Data shown represent the mean \pm SD of three biological replicates, each experiment is repeated three times. Data were analysed using one-way ANOVA followed by the Tukey's post hoc comparison test. Different letters above the bars indicate significant differences ($p < 0.05$). (AU = Arbitrary Units) Image collected and cropped by CiteAb from the following open publication (<https://pubmed.ncbi.nlm.nih.gov/31029157>), licensed under a CC-BY license. Not internally tested by Novus Biologicals.



Publications

Resetar M, Tietcheu Galani BR, Tsamo AT et al. Flindissone, a Limonoid Isolated from *Trichilia prieuriana*, Is an LXR Agonist *Journal of Natural Products* 2023-08-25 [PMID: 37526502] (WB, B/N)

Li J, Zhu Z, Li Y et al. D-4F, an apolipoprotein A-I mimetic, promotes the clearance of myelin debris and the reduction of foamy macrophages after spinal cord injury *Bioengineered* 2022-05-12 [PMID: 35546071]

Wiener JP, Desire S, Garliyev V et al. Down-Regulation of ABCA7 in Human Microglia, Astrocyte and THP-1 Cell Lines by Cholesterol Depletion, IL-1 β and TNF α , or PMA Cells 2023-08-25 [PMID: 37681876]

Wang H, Zheng A, Arias EB, Cartee GD. Prior AICAR induces elevated glucose uptake concomitant with greater β -AMPK activation and reduced membrane cholesterol in skeletal muscle from 26-month-old rats *Facets (Ott)* 2022-11-16 [PMID: 36381195]

Mao M, Deng Y, Wang L et al. Chronic unpredictable mild stress promotes atherosclerosis via adipose tissue dysfunction in ApoE(-/-) mice *PeerJ* 2023-09-04 [PMID: 37692113]

Huuska N, Netti E, Tulamo R et al. Serum Amyloid A Is Present in Human Saccular Intracranial Aneurysm Walls and Associates With Aneurysm Rupture *Journal of Neuropathology & Experimental Neurology* 2021-10-01 [PMID: 34534311] (IHC)

Xu (???) Y, Liu (??) C, Han (???) X et al. E17241 as a Novel ABCA1 (ATP-Binding Cassette Transporter A1) Upregulator Ameliorates Atherosclerosis in Mice *Arteriosclerosis, Thrombosis, and Vascular Biology* 2021-06-01 [PMID: 33441025]

Liu S, Zhang Y, Zheng X et al. Sulforaphane Inhibits Foam Cell Formation and Atherosclerosis via Mechanisms Involving the Modulation of Macrophage Cholesterol Transport and the Related Phenotype *Nutrients* 2023-04-28 [PMID: 37432260] (IHC-Fr, ICC/IF)

Molina-Gonzalez I, Holloway RK, Jiwaji Z et al. Astrocyte-oligodendrocyte interaction regulates central nervous system regeneration *Nature communications* 2023-06-08 [PMID: 37291151] (ICC/IF, Mouse)

Miyagawa S, Horie T, Nishino T et al. Inhibition of microRNA-33b in humanized mice ameliorates nonalcoholic steatohepatitis *Life science alliance* 2023-08-01 [PMID: 37263777] (WB, Mouse, Human)

Cao D, Khan Z, Li X et al. Macrophage angiotensin-converting enzyme (ACE) reduces atherosclerosis by increasing PPAR α and fundamentally changing lipid metabolism *Cardiovascular research* 2023-05-24 [PMID: 37225143] (WB, Mouse)

Yano H, Fujiwara Y, Horlad H et al. Blocking cholesterol efflux mechanism is a potential target for antilymphoma therapy *Cancer science* 2022-06-01 [PMID: 35343027] (WB, Human)

More publications at <http://www.novusbio.com/NB400-105>



Procedures

Western Blot protocol for ABCA1 Antibody (NB400-105)

RAW macrophages were treated with 9-cis-retinoic acid and 22R-hydroxycholesterol, known inducers of ABCA1 expression in macrophages. The total cell post-nuclear lysate (40ug protein) was separated by SDS-PAGE and detected using a 1:1000 dilution of NB400-105 affinity purified ABCA1 antibody incubated for 1 hour at room temperature. ABCA1 has been found to run as 3 bands by many researchers; this is probably due to protein modifications such as glycosylation.

NOTE: An important factor in detecting ABCA1 is in the cell type used. ABCA1 is expressed in very low levels in most cell types. Therefore, ABCA1 expression needs to be induced by using 22-hydroxycholesterol and 9-cis-retinoic acid as ligands for the transcription factor LXR.

1. Without heating at all (leave at room temp for about 15 to 20 minutes with Beta-mercaptoethanol), load 40 ug post-nuclear lysates* to 7.5% or 4-15% Tris-HCL SDS gel (Bio-RAD) in sample buffer. Do NOT boil the samples. (NP-40 will not interfere with the running of the protein on SDS-PAGE.)
2. Transfer to nitrocellulose membrane at 100V 1hr or 30V overnight.
3. Block membrane in 5% milk in TBS-T for at least 1 hr. Wash with TBS-T 5 minutes.
4. Blot with anti-ABCA1 antibody in 3% milk in TBS-T for 1 hour.
5. Wash with TBS-T 3 times, 10 minutes each.
6. Blot with anti-rabbit secondary according to the recommended dilutions in 3% milk in TBS-T for 1 hour.
7. Wash with TBS-T 3 times, 10 minutes each.
8. Detect with chemiluminescent reagent (Pierce).
9. Image

TBS-T: Tris-buffered-saline with Tween-20

See also the specific references mentioned in the datasheet. *Post-nuclear lysate is the result of sonication or dounce homogenization of lysate, centrifugation at low-speed, and the removal of nuclei. The resulting supernatant is called post-nuclear and contains cytosolic and membrane proteins without any of the nuclear components.

Immunohistochemistry-Paraffin protocol for ABCA1 Antibody (NB400-105)

ABCA1 Antibody:

Immunohistochemistry-Formalin Fixed Paraffin Embedded sections

I. Deparaffinization:

- A. Treat slides with Xylene: 3 changes for 5 minutes each. Drain slides for 10 seconds between changes.
- B. Treat slides with 100% Reagent Alcohol: 3 changes for 5 minutes each. Drain slides for 10 seconds between changes.

II. Quench Endogenous Peroxidase:

- A. Place slides in peroxidase quenching solution: 15-30 minutes.

To Prepare 200 ml of Quenching Solution:

-Add 3 ml of 30% Hydrogen Peroxide to 200 ml of Methanol.

-Use within 4 hours of preparation

- B. Place slides in distilled water: 2 changes for 2 minutes each.

III. Retrieve Epitopes:

- A. Preheat Citrate Buffer. Place 200 ml of Citrate Buffer Working Solution into container, cover and place into steamer. Heat to 90-96 degrees C.
- B. Place rack of slides into hot Citrate Buffer for 20 minutes. Cover.
- C. Carefully remove container with slides from steamer and cool on bench, uncovered, for 20 minutes.
- D. Slowly add distilled water to further cool for 5 minutes.
- E. Rinse slides with distilled water. 2 changes for 2 minutes each.

IV. Immunostaining Procedure:

- A. Remove each slide from rack and circle tissue section with a hydrophobic barrier pen (e.g. Liquid Blocker-Super Pap Pen).
- B. Flood slide with Wash Solution. Do not allow tissue sections to dry for the rest of the procedure.

- C. Drain wash solution and apply 4 drops of Blocking Reagent to each slide and incubate for 15 minutes.
- D. Drain Blocking Reagent (do not wash off the Blocking Reagent), apply 200 ul of Primary Antibody solution to each slide, and incubate for 1 hour.
- E. Wash slides with Wash Solution: 3 changes for 5 minutes each.
- F. Drain wash solution, apply 4 drops of Secondary antibody to each slide and incubate for 1 hour.
- G. Wash slides with Wash Solution: 3 changes for 5 minutes each.
- H. Drain wash solution, apply 4 drops of DAB Substrate to each slide and develop for 5-10 minutes. Check development with microscope.
- I. Wash slides with Wash Solution: 3 changes for 5 minutes each.
- J. Drain wash solution, apply 4 drops of Hematoxylin to each slide and stain for 1-3 minutes. Increase time if darker counterstaining is desired.
- K. Wash slides with Wash Solution: 2-3 changes for 2 minutes each.
- L. Drain wash solution and apply 4 drops of Bluing Solution to each slide for 1-2 minutes.
- M. Rinse slides in distilled water.
- N. Soak slides in 70% reagent alcohol: 3 minutes with intermittent agitation.
- O. Soak slides in 95% reagent alcohol: 2 changes for 3 minutes each with intermittent agitation.
- P. Soak slides in 100% reagent alcohol: 3 changes for 3 minutes each with intermittent agitation. Drain slides for 10 seconds between each change.
- Q. Soak slides in Xylene: 3 changes for 3 minutes each with intermittent agitation. Drain slides for 10 seconds between each change.
- R. Apply 2-3 drops of non-aqueous mounting media to each slide and mount coverslip.
- S. Lay slides on a flat surface to dry prior to viewing under microscope.

NOTES:

- Use treated slides (e.g. HistoBond) to assure adherence of FFPE sections to slide.
 - Prior to deparaffinization, heat slides overnight in a 60 degrees C oven.
 - All steps in which Xylene is used should be performed in a fume hood.
- For Epitope Retrieval, a microwave or pressure cooker may be substituted for the steamer method. Adjust times as necessary depending on conditions.
- For the initial IHC run with a new primary antibody, test tissues with and without Epitope Retrieval. In some instances, Epitope Retrieval may not be necessary.
 - 200 ul is the recommended maximum volume to apply to a slide for full coverage. Using more than 200 ul may allow solutions to wick off the slide and create drying artifacts. Small tissue sections less than 200 ul may be used.
 - 5 minutes of development with DAB Substrate should be sufficient. Do not develop for more than 10 minutes. If 5 minutes of development causes background staining, further dilution of the primary antibody may be necessary.
- Hematoxylin should produce a light nuclear counterstain so as not to obscure the DAB staining. Counterstain for 1-1.5 minutes for nuclear antigens. Counterstain for 2-3 minutes for cytoplasmic and membranous antigens. If darker counterstaining is desired increase time (up to 10 minutes).



Novus Biologicals USA

10730 E. Briarwood Avenue
Centennial, CO 80112
USA
Phone: 303.730.1950
Toll Free: 1.888.506.6887
Fax: 303.730.1966
nb-customerservice@bio-techne.com

Bio-Techne Canada

21 Canmotor Ave
Toronto, ON M8Z 4E6
Canada
Phone: 905.827.6400
Toll Free: 855.668.8722
Fax: 905.827.6402
canada.inquires@bio-techne.com

Bio-Techne Ltd

19 Barton Lane
Abingdon Science Park
Abingdon, OX14 3NB, United Kingdom
Phone: (44) (0) 1235 529449
Free Phone: 0800 37 34 15
Fax: (44) (0) 1235 533420
info.EMEA@bio-techne.com

General Contact Information

www.novusbio.com
Technical Support: nb-technical@bio-techne.com
Orders: nb-customerservice@bio-techne.com
General: novus@novusbio.com

Products Related to NB400-105

NBP1-30159	Raw 264.7 Whole Cell - T0901317 treated Assay Kit
NB400-105PEP	ABCA1 Antibody Blocking Peptide
HAF008	Goat anti-Rabbit IgG Secondary Antibody [HRP]
NB7160	Goat anti-Rabbit IgG (H+L) Secondary Antibody [HRP]
NBP2-24891	Rabbit IgG Isotype Control

Limitations

This product is for research use only and is not approved for use in humans or in clinical diagnosis. Primary Antibodies are guaranteed for 1 year from date of receipt.

For more information on our 100% guarantee, please visit www.novusbio.com/guarantee

Earn gift cards/discounts by submitting a review: www.novusbio.com/reviews/submit/NB400-105

Earn gift cards/discounts by submitting a publication using this product:
www.novusbio.com/publications

